

IDENTIFICATION OF LOCAL ELASTIC PARAMETERS IN HETEROGENEOUS MATERIALS USING A PARALLELIZED FEMU METHOD

L. PETUREAU*, P. DOUMALIN and F. BREMAND
Photomechanics & Experimental Mechanics (PEM) team
Dept. Génie Mécanique et Systèmes Complexes (GMSC)
Institut P' UPR 3346 CNRS - Université de Poitiers – ENSMA
SP2MI – Téléport 2, 11 Boulevard Marie et Pierre Curie
BP 30179, F86962 Futuroscope Chasseneuil Cedex, FRANCE
E-mails: louis.petureau@univ-poitiers.fr
pascal.doumalin@univ-poitiers.fr; fabrice.bremmand@univ-poitiers.fr

In this work, we explore the possibilities of the widespread Finite Element Model Updating method (FEMU) in order to identify the local elastic mechanical properties in heterogeneous materials. The objective function is defined as a quadratic error of the discrepancy between measured fields and simulated ones. We compare two different formulations of the function, one based on the displacement fields and one based on the strain fields. We use a genetic algorithm in order to minimize these functions. We prove that the strain functional associated with the genetic algorithm is the best combination. We then improve the implementation of the method by parallelizing the algorithm in order to reduce the computation cost. We validate the approach with simulated cases in 2D.

Key words: identification - elasticity - heterogeneous material - genetic algorithm - parallel computation.

1. Introduction

Thanks to low-cost optical devices enabling 2D and 3D displacement fields measurements, identification of material properties based on the full-field measurement method, has become very popular. Especially, digital image correlation (DIC) consists of a sampling of the displacement fields over a surface or within a volume of the sample on a regular grid is most frequently used. The identification approach is a particular case of inverse problem which aims to identify the map of material properties that underlies the experimental measurements.

An abundant literature exists on the identification of linear and non-linear constitutive equation parameters but materials are generally assumed to be homogeneous [1], [2], [3], [4]. In the last decade, the need to identify mechanical properties in heterogeneous materials has become an active research domain in order to better understand these complex mechanical behaviors. Indeed, the identification allows to mechanically characterize the materials to eventually know the stress fields. In this way, the entire constitutive equation is known and not just the kinematic part. In this work, we focus on the identification of global isotropic linear elastic but heterogeneous behaviors at a global scale.

Until now, five well-known identification techniques have been proposed: the virtual field method (VFM) proposed by [5], the constitutive equation gap method (CEGM) proposed by [6], the reciprocity gap method (RGM) proposed by [7], the equilibrium gap method (EGM) proposed by [8] and the finite element model updating method (FEMUM) proposed by [9]. All of these methods have been extensively used to identify global mechanical parameters, recent overviews compared them to build an optimal framework [10]

* To whom correspondence should be addressed

and to evaluate their performances in elastic and elasto-plastic identifications [11]. Widespread variants of these methods are vibration-based methods as in [12] where the authors identified orthotropic properties of plates. In order to identify local mechanical parameters where the homogeneous hypothesis is not verified, some of these methods have been modified to be adapted to heterogeneous materials. The Fourier series-based VFM [13] and the constitutive compatibility method (CCM) [14], based on a reformulation of CEGM, are examples of recent developments in this area. As far as we know, there is no work in the literature which has tested the FEMU method in this case. Thus, we intend here to explore the possible application of this method to identify local parameters in the case of heterogeneous materials.

In the first part, we recall the classical definition of an identification problem with the governing equations. Then, we describe the principle of the FEMU method and we detail the finite element method equations for our method and the chosen minimization algorithm, the genetic algorithm. The third part presents the parallelization of the algorithm, which allows us to save computation time. Finally, the last part presents simulated cases in 2D to validate the approach and shows the capabilities of the method to identify local elastic parameters.

2. Identification problem

2.1. Governing equations

Let us suppose an elastic solid, see Fig.1, which lies in the domain Ω in the undeformed configuration. This domain is subjected to the prescribed strength field \bar{T} over the boundary part $\Gamma_{\bar{T}}$ and the prescribed displacement field \bar{u} over the boundary part $\Gamma_{\bar{u}}$. The domain Ω is assumed to be a heterogeneous isotropic elastic material. Three sets of differential equations govern this elastic problem:

- The kinematics compatibility equations of the strain-displacement relation and the compatibility with the prescribed field \bar{u}

$$\varepsilon[\mathbf{u}] = \frac{1}{2}(\nabla^T \mathbf{u} + \nabla \mathbf{u}) \quad \text{in } \Omega, \quad (2.1)$$

$$\mathbf{u} = \bar{\mathbf{u}} \quad \text{over } \Gamma_{\bar{u}} \quad (2.2)$$

where ∇ and ∇^T are, respectively, the gradient operator and its transpose, and ε - the linearized Green-Lagrange strain tensor.

- The equilibrium equations consisting of the interior equilibrium of the domain, assuming no body forces, and the equilibrium with the prescribed field \bar{T}

$$\text{div } \boldsymbol{\sigma} = \mathbf{0} \quad \text{in } \Omega, \quad (2.3)$$

$$\boldsymbol{\sigma} \cdot \mathbf{n} = \bar{\mathbf{T}} \quad \text{over } \Gamma_{\bar{T}} \quad (2.4)$$

where div is the divergence operator, \mathbf{n} - the external unit vector normal to $\Gamma_{\bar{T}}$ and $\boldsymbol{\sigma}$ - the Cauchy stress tensor.

- The constitutive equation consisting of the stress-strain relation

$$\boldsymbol{\sigma} = \mathcal{A}(\boldsymbol{\theta}) : \varepsilon[\mathbf{u}] \quad (2.5)$$

where \mathcal{A} denotes the fourth order elasticity tensor depending on the elastic parameters $\boldsymbol{\theta}$.

These equations are used to solve a direct problem which consists of computing the mechanical fields of the domain governed by a constitutive equation and are subjected to prescribed quantities. These fields can be kinematics fields, such as displacement and strain fields, or stress fields. This is usually done by using the finite element method.

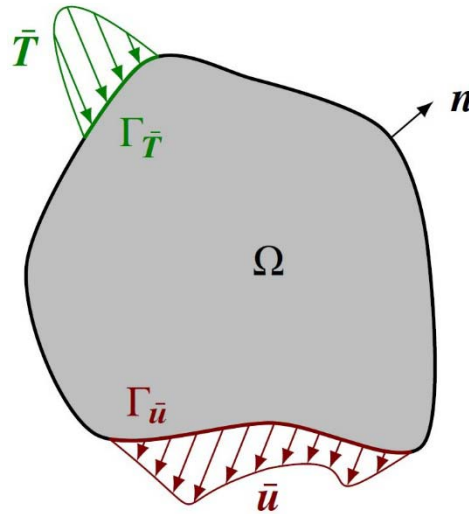


Fig.1. Elastic domain subjected to non-overlapping static and kinematic boundary conditions.

2.2. Identification problem

An identification problem consists in inverting the direct problem in order to retrieve the parameters θ of the constitutive equation which drive to the measured mechanical fields. The measurements are usually done with a full-field measurement technique such as digital image correlation. It allows us to measure displacement fields at discrete locations on a grid. Thus, strain fields can be deduced afterwards. So, we experimentally have access to the kinematic fields.

The identification problem aims to provide values for the mechanical parameters of the constitutive equation. We have to find θ in a way that Eqs (2.1), (2.2), (2.3) and (2.4) are satisfied through the constitutive Eq.(2.5).

3. Finite element model updating method

3.1. Principle of the method

The FEMU method is based on overdetermined full-field measurements to identify material constitutive parameters. The principle of the method, illustrated in Fig.2, consists of iteratively updating the material constitutive parameters of a finite element model in order to minimize a functional based on measured fields and simulated fields with an adequate minimization algorithm.

In this study, we use two different functionals, J_u expressed as a function of displacement fields

$$J_u = \frac{1}{2} \sum_i^n (u_i^{exp} - u_i^{sim}(\theta))^2, \quad (3.1)$$

and J_E expressed as a function of Green-Lagrange strain fields

$$J_E = \frac{1}{2} \sum_i^n \left(E_i^{exp} - E_i^{sim}(\boldsymbol{\theta}) \right)^2 \quad (3.2)$$

where n is the total number of measured points and $\boldsymbol{\theta}$ is the vector gathering the unknown material constitutive parameters. u_i^{exp} and E_i^{exp} are, respectively, the measured displacements and strains obtained by DIC and u_i^{sim} and E_i^{sim} are, respectively, the simulated displacements and strains obtained by the finite element model. These two functionals are compared in order to select the one that fits better for identification of local mechanical parameters.

In this work, we use the isotropic linear-elasticity constitutive equation which can be expressed as follows with Lamé's parameters

$$\boldsymbol{\sigma} = \lambda \text{tr}(\boldsymbol{\varepsilon}) \mathbf{I} + 2\mu \boldsymbol{\varepsilon}. \quad (3.3)$$

Numerically, Young's modulus E and Poisson's coefficient ν are preferred to Lamé's parameters. One should note that ν is considered fixed and constant in the materials for all cases in this work because it can be determined experimentally with the ratio between the transverse strain and the normal strain.

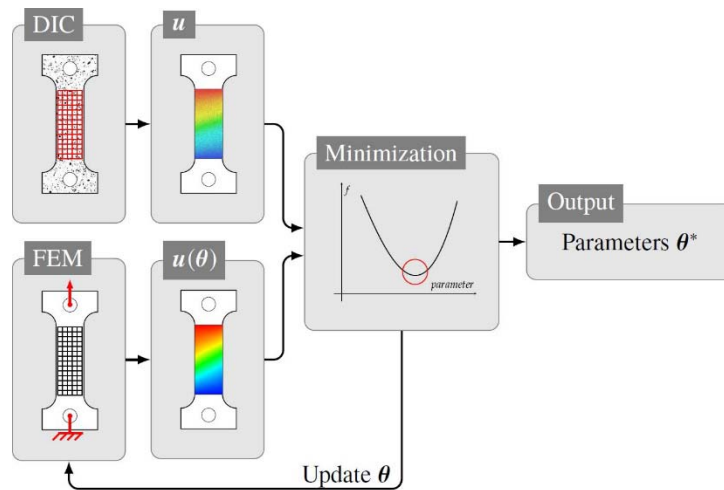


Fig.2. Principle of the FEMU method.

3.2. Finite element model

The virtual work principle makes it possible to write the weak formulation of the direct problem governed by the Eqs (2.1) to (2.5)

$$\int_{\Omega} \boldsymbol{\varepsilon}^*[u^*] : \mathcal{A}(\boldsymbol{\theta}) : \boldsymbol{\varepsilon}[u] dV = \int_{\Gamma_{\bar{T}}} \bar{\mathbf{T}} \cdot \mathbf{u}^* dS. \quad (3.4)$$

Generally, the finite element method is used to solve this problem. The finite element procedure is implemented in an in-house C code and is based on the classical finite element equations. In this work, we use a linear Lagrange finite element in 2D which has four nodes, see Fig.3. The mesh of the model is constructed in such a way that each node corresponds to each measured point. With this approach, we ensure a compatibility between the experimental fields and the simulated ones. As a consequence, the mesh is a

regular grid with a constant gap between the nodes like the correlation grid. We briefly resume the equations of the finite element method.

The elementary rigidity matrix $[K^e]$ of an element e of the mesh can be written

$$[K^e] = \int_V [B^e]^T [D^e] [B^e] dV \quad (3.5)$$

where $[B^e]$ is the shape function derivative matrix of the element e and $[D^e]$ is the constitutive equation matrix for the volume V of the element e which is a function of the unknown mechanical parameters and can be expressed in 2D plane stress

$$[D^e] = \frac{E}{1-\nu^2} \begin{bmatrix} 1 & \nu & 0 \\ \nu & 1 & 0 \\ 0 & 0 & \frac{1-\nu}{2} \end{bmatrix}. \quad (3.6)$$

The elementary force vector $\{F^e\}$ of the element e of the mesh can be written

$$\{F^e\} = \int_S [N^e]^T \{T^e\} dS \quad (3.7)$$

where $\{T^e\}$ is the external force vector applied to the surface S of the element e and $[N^e]$ is the shape function matrix of the element e .

Once all the elementary quantities $[K^e]$ and $\{F^e\}$ are computed, we can assembly them into global quantities $[K]$ and $\{F\}$

$$[K] = \sum_e [L^e]^t [K^e] [L^e], \quad (3.8)$$

$$\{F\} = \sum_e [L^e]^t \{F^e\} \quad (3.9)$$

where $[L^e]$ is the localization matrix of the element e in the mesh.

Before the resolution, boundary conditions have to be applied to the system. We do this in a way that preserves the symmetry of $[K]$.

The solution of the finite element problem, the simulated displacement field $\{\mathbf{u}^{sim}\}$, consists of resolving the following linear system

$$[K]\{\mathbf{u}^{sim}\} = \{F\}. \quad (3.10)$$

Different algorithms can solve this system but the preconditioned conjugate gradient method is particularly adapted in this case because $[K]$ is symmetric and sparse.

The strains are computed using a classical finite difference scheme. This choice is motivated by the fact that it is the same technique as the one used for experimental strain calculation.

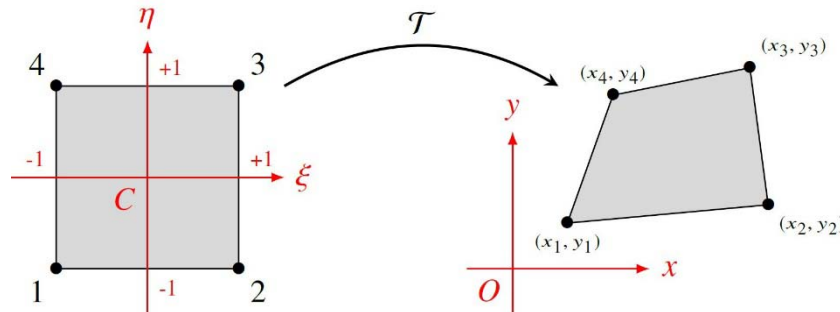


Fig.3. 2D linear Lagrange element.

3.3. Minimization algorithm

Standard gradient based minimization algorithms cannot be selected in our case. The unknowns are structure-dependant because the derivative of the functional for one mechanical parameter does not keep its sign constant when the other parameters change. It means that the derivative cannot be trusted to guide the algorithm so we need to use non-gradient based minimization methods.

We select the genetic algorithm because it has been applied to many different problems and has the advantage to converge quickly to the global optimum. The authors used it in [15] to identify the Mooney-Rivlin parameters of hyperelastic materials. Its disadvantage is that it requires many generations to reach the global optimum. The genetic algorithm belongs to evolutionary strategies to solve optimization problems. It has been developed in the 1970s and is based on the natural selection mechanisms [16]. The main idea is to define a randomly distributed initial population and to apply some genetic operators to adapt the population to the functional of the problem, see Fig.4.

We briefly describe these operators:

- ranking: it assigns a fitness value to the individuals which consists in a linear application of the objective function ;
- selection: this step consists in choosing the best individuals of the population. Different techniques have been developed [17], in this work we choose the roulette wheel selection [18]. It can be seen as a wheel in which each individual occupies a surface proportional to its fitness value, see Fig.5a;
- crossover: this is done by combining some genes of two individuals, called parents. We use the uniform crossover technique which consists in selecting some genes of the parents following a distribution, see Fig.5b. A review of the different techniques for crossover operator can be found in [19];
- mutation: this step modifies a gene of an individual. The probability that this operator occurs is usually small $P_{mut} = 1\%$. The mutation is illustrated in Fig.5c;
- convergence criterion: we do not define a specific criterion, the algorithm iterates until the maximum number of generations is reached.

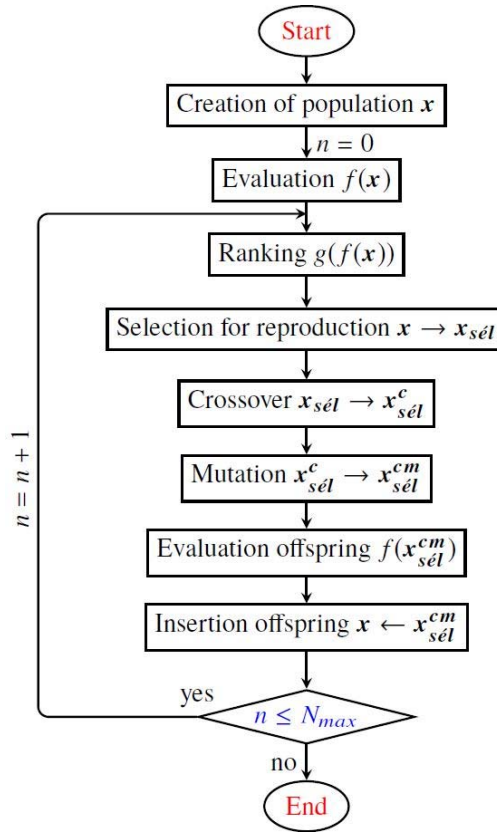


Fig.4. Principle of the genetic algorithm.

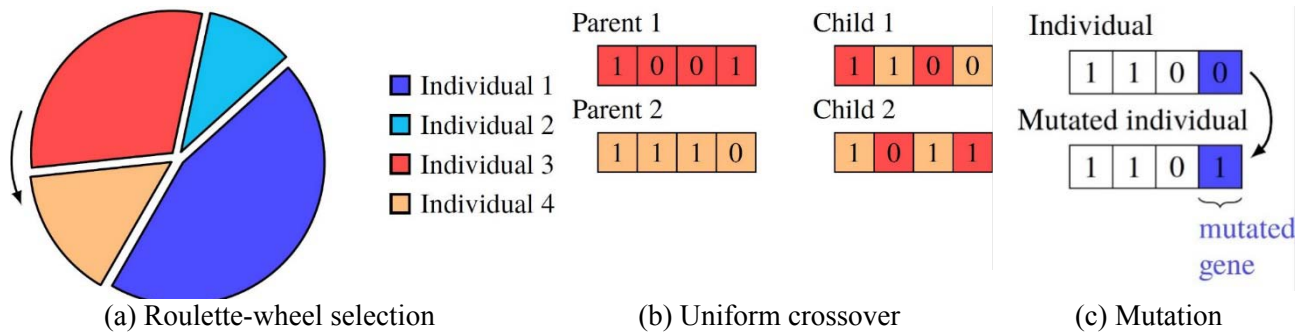


Fig.5. Illustration of the genetic algorithm operators.

4. Parallel implementation

Because of the iterative process of the FEMU method, it can be time consuming. Therefore, in order to reduce the computation time, we chose to parallelize the genetic algorithm. Several different parallel genetic algorithms are available [20] but we selected the master-slave model (MSM), see Fig.6, because it renders it possible to get a significant speed-up of the process without having to modify much of the algorithm.

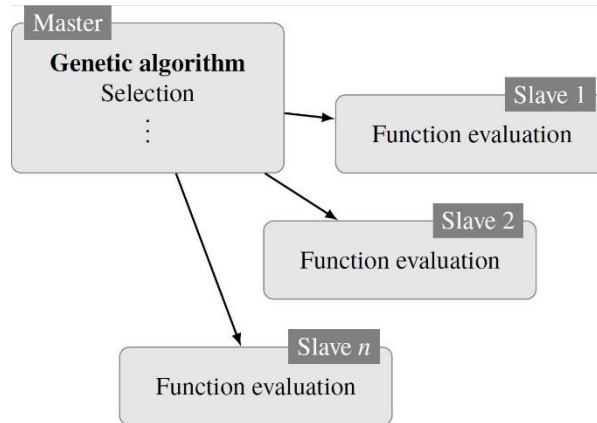


Fig.6. Master-slave model.

4.1. Master-slave parallel genetic algorithm

In this model, all genetic operators are done in the master processor. The most common operation that is parallelized to slave processors is the objective function evaluation because it only requires the knowledge of the individual being evaluated so there is no need to communicate during this phase. In our case, it is particularly adapted because the evaluation of the objective function consists of solving the finite element linear system (15) which can be time consuming when the number of nodes increases.

A fraction of the population is sent to the slave processors to evaluate some individuals of the population. The MSM is implemented as synchronous, meaning that the master waits for all slave processors to return their results before continuing the minimization process. So basically, it works exactly like a simple genetic algorithm.

4.2. Message passing interface paradigm

To implement this parallel architecture of the genetic algorithm, we used the Message Passing Interface (MPI) paradigm, which is the most common way to do parallel computation for distributed-memory computers [21]. All processors form a network and specific communication functions allow us to communicate between these processors, see Fig.7. The program is written in C code and calculations have been performed on the supercomputer facilities of the University of Poitiers (Mésocentre de calcul de Poitou-Charentes).

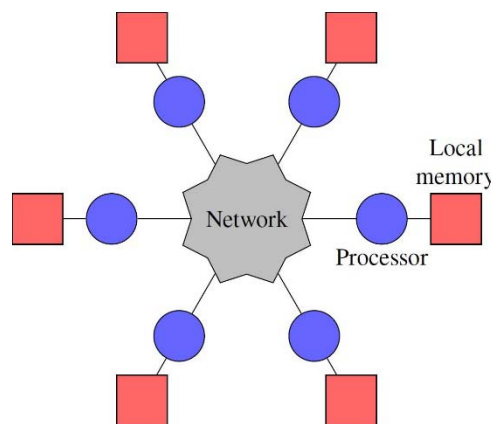


Fig.7. Distributed-memory principle.

In order to have the best speed-up factor, we balance the computation load over the processors in such a way that slave processors have the same amount of calculations and that the master processor is slightly underloaded compared to the slave processors.

5. Simulated tests

5.1. Description of tests

Here, we consider a reference problem in order to validate the approach described above. The distribution of Young's modulus and the boundary conditions of the elastic problem are shown in Fig.8. Three different areas with three different Young's modulus values define the mechanical properties field. The Poisson's coefficient is fixed to $\nu = 0.3$. This case is particularly adapted to evaluate the method when mechanical properties are constant in some regions and suddenly vary in other regions.

The reference problem was solved using a finite element solver called Cast3M [22]. The displacement fields solution of this problem is used as experimental data.

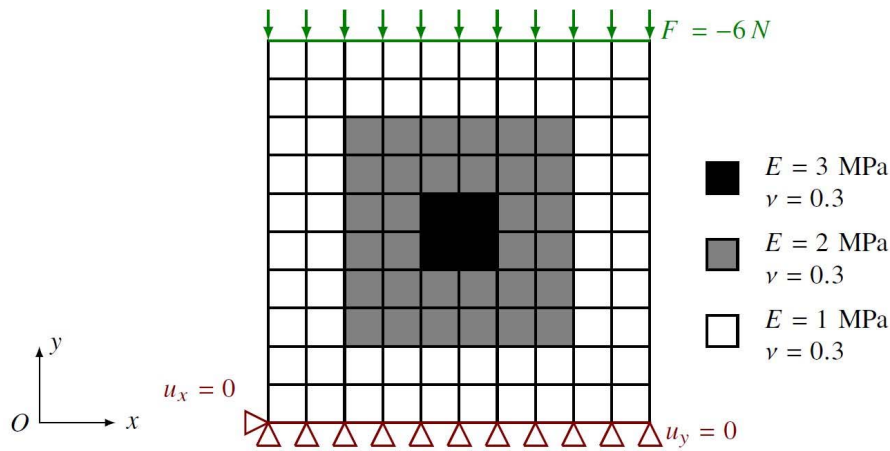


Fig.8. Reference problem in 2D.

5.2. Results with no noise

In this section, the displacement fields of the reference case are given to the identification method with no noise added. The FEMU method is applied successively 10 times on the reference case described above. The size of the population of the genetic algorithm is equal to 15 individuals per unknown and iterates during 10000 generations. The number of selected individuals represent 93% of the complete population. The probability for an individual to mutate is fixed to 1%. For these parameters, a non-parallel program would take approximatively 13 hours. Using the supercomputer facilities and our parallelized code on 100 cores, it takes around 10 minutes. The speed-up factor is about 80, which is a huge improvement of the computation time. We clearly see the advantage of this approach.

Figure 9 shows the average identified Young's modulus for the 10 identifications and their relative gaps for the two different functionals. We observe that the results with the J_E functional are better than those with the J_u functional. The different mechanical areas are well reconstructed in both cases but there is less dispersion with the J_E functional. If we look at the relative error between the reference and identified values of Young's modulus in Fig.9, the same remark can be made. We can add that the values of relative error for J_U vary 30% and are higher than those for J_E which vary 10%. Moreover, we remark that the relative errors increase when elements are close to the inner boundary and conversely the errors are decreasing when the elements are close to the upper boundary where the load is applied. It indicates that

elements which are more deformed are easier to identify in comparison with those which have weak values of displacements/strains.

Figure 10 shows the mean kinematics residuals of the 10 identifications at the end of the process. As previously, residuals are weaker for the J_E functional for all kinematic fields.

Figure 11 shows the mean evolution of the best individual f_{min} during the identification process for the two different functionals and for the 10 identifications. In order to do a fair comparison between these functionals, the values of the objective functions are normalized by the maximum value $\max(f_{min})$ for each of them. Then, the values vary between 0 and 1. We see that the J_E functional converges very quickly and faster than J_u during the first thousand generations. At the process end, the convergence speed is the same for both functionals but is quite slow compared to the beginning of the process.

Figure 12 shows the evolution of the best individual for the element 22 for the two functionals. We chose these particular evolutions because the identified values of Young's modulus are the worst for the two functionals. These evolutions show that the J_E functional continues to converge towards the reference value but this is not the case for the J_u functional. We can see that it almost stops to converge around the generation 2000. As we noticed before, the convergence is quite slow at the end of the process. We observe that from the generation 1000 to the end, the improvement in the values is weak, so we can think about the reduction of the maximum number of generations. The choice is up to the user: if one reduces this number, there will potentially be an increase of the errors in the identified values but the process will be faster.

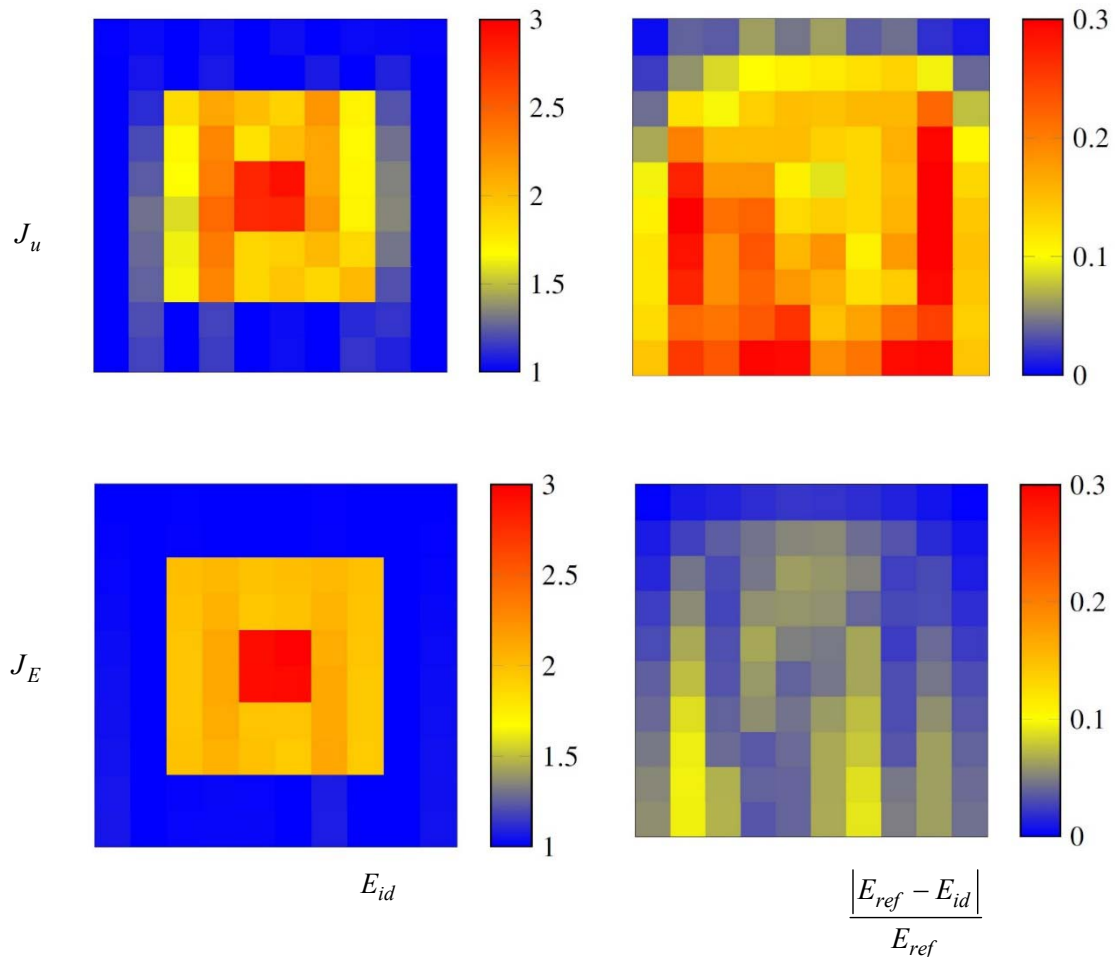


Fig.9. Identified Young's modulus and mean relative errors.

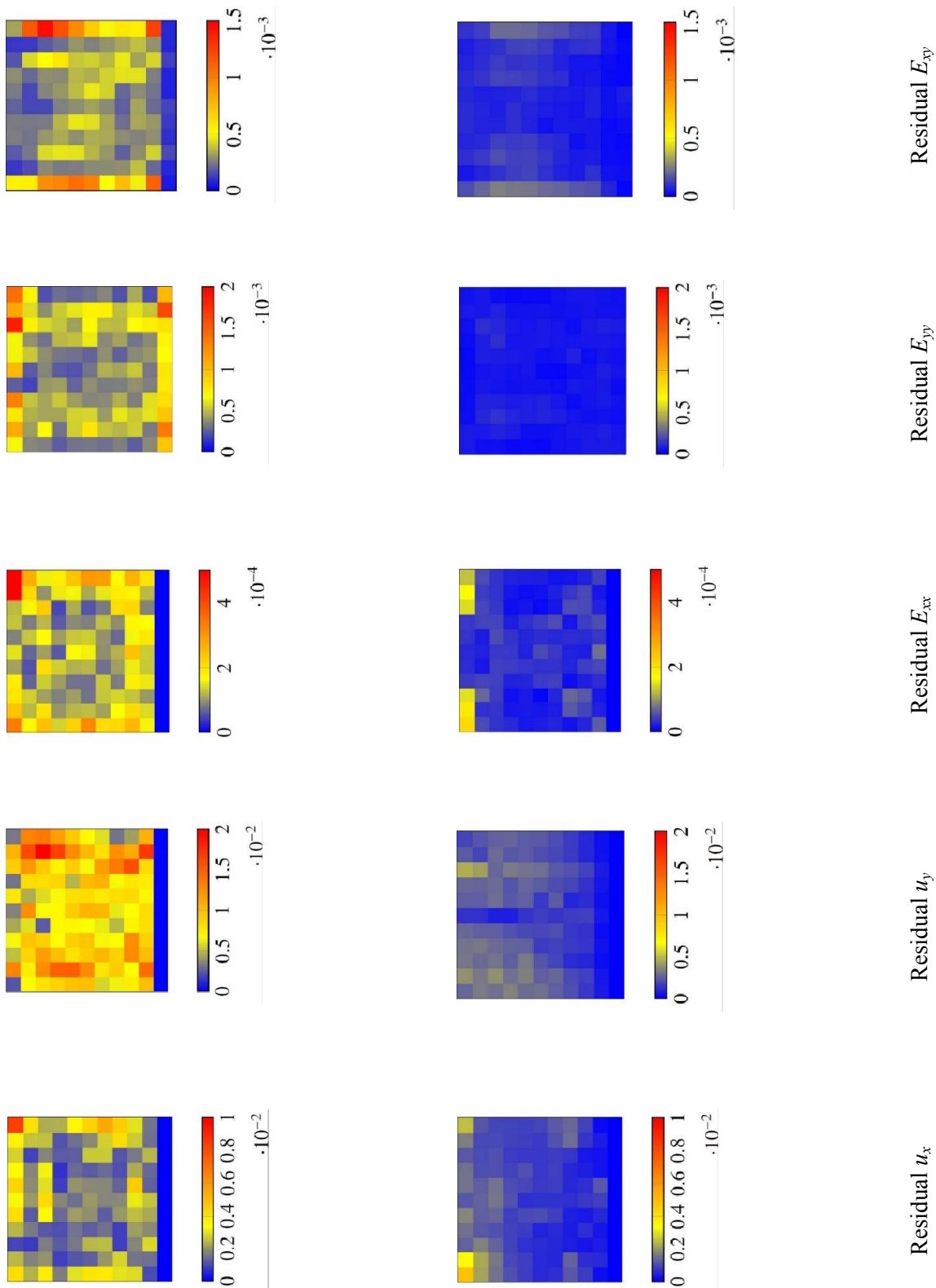


Fig.10. Kinematic residuals for the two functionals of the FEMU method.

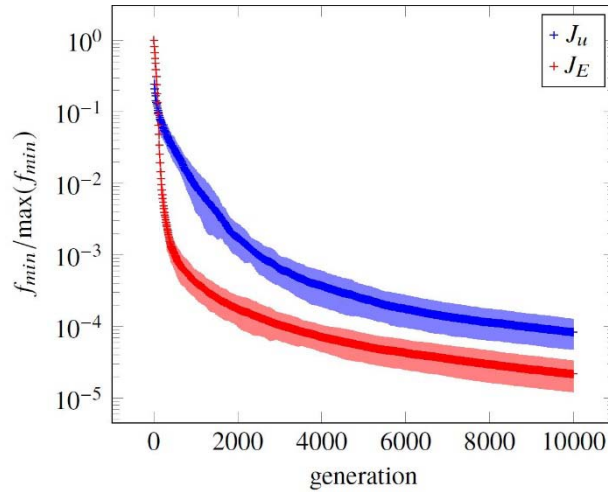


Fig.11. Mean best individual evolution for the two functionals for 10 identifications.

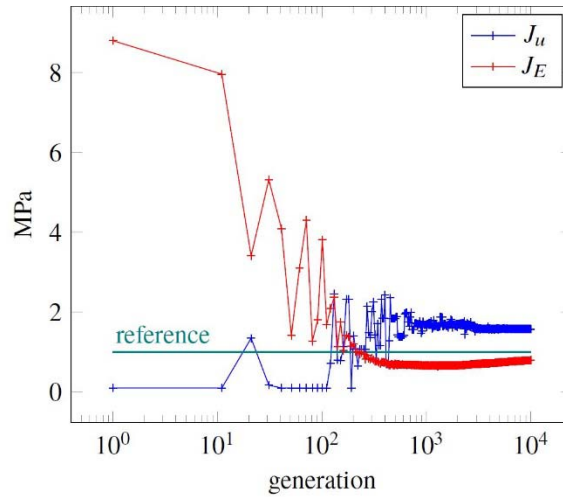


Fig.12. Evolution of the best individual for the element 22 for the two functionals.

5.3. Influence of noise

In this section, a numerical noise is added to the displacement fields of the reference case in order to evaluate the performances of the method when data are noisy. This is done with the following formula

$$u_{x,y}^{noise} = u_{x,y}^{ref} \cdot r \cdot a \quad (5.1)$$

where r is a normally distributed random number with zero mean and a unit standard deviation, a is the amplitude of noise expressed in millimeters. We test the identification method for four values of noise amplitude $a = 0.01mm$ to $a = 0.04mm$. These values typically are the values of DIC measurement errors. In the same manner as we did before for the reference case, we did successively 10 identifications for each noise amplitude.

Figure 13 shows the mean relative errors on the values of identified Young's moduli. We clearly see the influence of noisy data on the identification process. Indeed, results for the J_u functional show that it is less sensitive to noise compared to the results for J_E . This is an expected observation because the strain calculation consists basically on the derivation of displacement fields. So, it can be seen as a high-pass filter.

It means that small variations of displacements will be increased by the strain calculation scheme. It explains that the J_E functional is more sensitive to noise. Nevertheless, we observe that this functional has still better results than the other one.

Figures 14 and 15, respectively, show the mean identified Young's modulus, with the relative errors, and the mean kinematic residuals for the 10 identifications for the two functionals for a noise amplitude $a = 0.02mm$. We observe that the results are better in terms of identified values with weaker relative errors. Nevertheless, for the reconstructed kinematic fields, we see that the residuals are quite similar for both functionals. This observation added to the previous one indicates that the J_E functional provides better results with similar errors in the kinematic fields. It motivates once again the use of this functional for experimental cases.

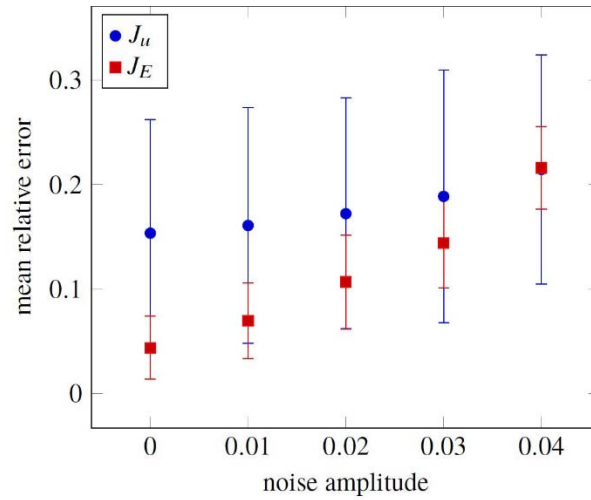


Fig.13. Mean identified values for different levels of noise.

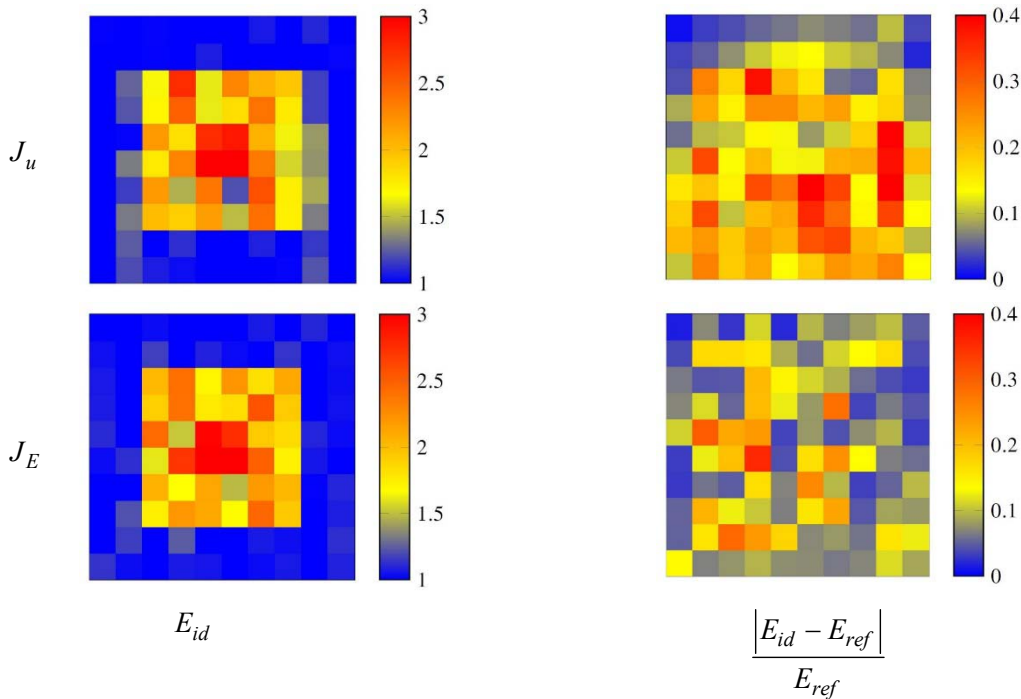


Fig.14. Identified Young's modulus for a noise amplitude $a=0.02$.

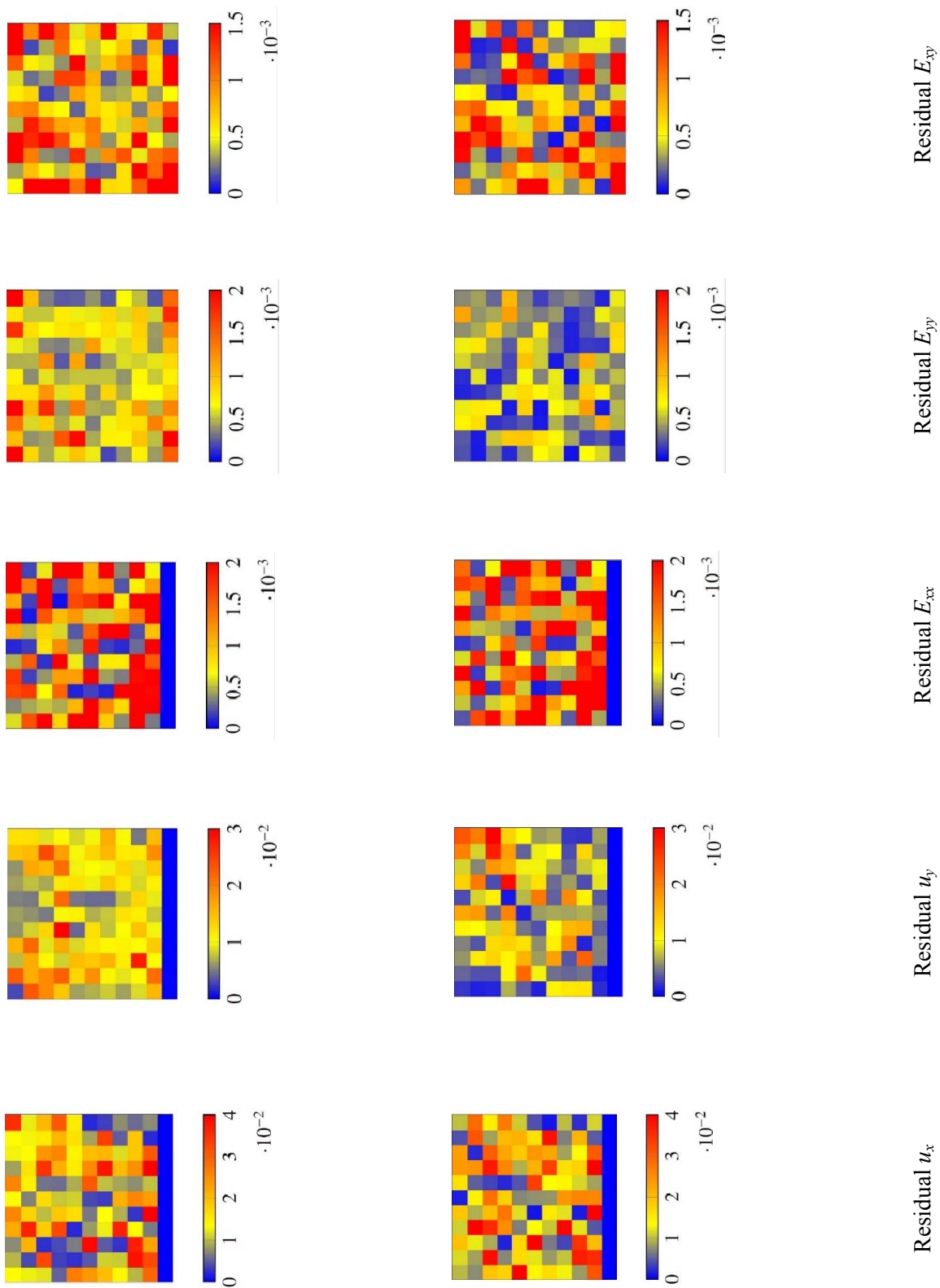


Fig.15. Kinematic residuals for the two functionals of the FEMU method for a noise amplitude $a=0.02$.

6. Concluding remarks

In this study, we have explored the capability of the FEMU method to identify local mechanical elastic parameters. The classical implementation of this method is done for homogeneous materials, so for very few mechanical parameters. Here, we have implemented it using a non-gradient minimization algorithm, genetic algorithm, which is more robust and efficient in the case of many unknown parameters. The inconvenience of this method is its iterative formalism which can be very time consuming in computations. In order to reduce this issue, we have proposed a master-slave parallel implementation of the algorithm. This new implementation is very efficient and we have achieved a high speed-up factor around 80. We have shown on a simulated case, with or without noise, that the method can provide local differences of mechanical behavior in heterogeneous materials. We compared a functional based on displacements and another one based on strains. The one based on strains allows a faster convergence and better identification of moduli with less disparity than the one based on displacements.

These promising results offer some interesting perspectives for the characterization and the understanding of mechanical behavior of heterogeneous materials. We are currently working on some in-plane experimental applications of this method. Some recent work, such as [23], show that hybrid OpenMP/MPI parallel computing can be even more efficient than pure MPI, it could be a promising perspective to reduce the execution time of our method.

Nomenclature

- \mathcal{A} – fourth order elasticity tensor
- a – amplitude of noise expressed in millimeters
- $[B^e]$ – shape function derivative matrix of the element e
- $[D^e]$ – constitutive equation matrix of the element e
- E_i^{exp} – measured Green-Lagrange strains obtained by DIC
- E_i^{sim} – simulated Green-Lagrange strains obtained by the finite element model
- $\{F\}$ – global force vector for all elements
- $\{F^e\}$ – elementary force vector of the element e
- f_{min} – value of the functional of the best individual of the population of the genetic algorithm
- J_E – functional expressed as a function of Green-Lagrange strain fields
- J_u – functional expressed as a function of displacement fields
- $[K]$ – global rigidity matrix for all elements
- $[K^e]$ – elementary rigidity matrix of element e
- $[L^e]$ – localization matrix of the element e
- $[N^e]$ – shape function matrix of the element e
- \mathbf{n} – the external unit vector normal to $\Gamma_{\bar{T}}$
- r – normally distributed random number with zero mean and a unit standard deviation
- $\bar{\mathbf{u}}$ – prescribed displacement field
- \bar{T} – prescribed strength field
- $\{T^e\}$ – external force vector applied to the surface of the element e
- u_i^{exp} – measured displacements obtained by DIC
- u_i^{sim} – simulated displacements obtained by the finite element model
- $\Gamma_{\bar{T}}$ – boundary part of Ω with prescribed strength field \bar{T}
- $\Gamma_{\bar{\mathbf{u}}}$ – boundary part of Ω with prescribed displacement field $\bar{\mathbf{u}}$

- ε – linearized Green-Lagrange strain tensor
- θ – elastic parameters
- λ, μ – Lamé's parameters
- σ – the Cauchy stress tensor
- Ω – domain of the solid in the undeformed configuration

References

- [1] Merzouki T., Nouri H and Roger F. (2014): *Direct identification of nonlinear damage behavior of composite materials using the constitutive equation gap method.* – International Journal of Mechanical Sciences, vol.89, pp.487-499.
- [2] Passieux J.-C., Bugarin F., David C., Périé J.-N. and Robert L. (2014): *Multiscale displacement field measurement using digital image correlation: application to the identification of elastic properties.* – Experimental Mechanics, vol.55, No.1, pp.121-137.
- [3] Azzouna M.B., Feissel P. and Villon P. (2015): *Robust identification of elastic properties using the modified constitutive relation error.* – Computer Methods in Applied Mechanics and Engineering, vol.295, pp.196-218.
- [4] He T., Liu L. and Makeev A. (2018): *Uncertainty analysis in composite material properties characterization using digital image correlation and finite element model updating.* – Composite Structures, vol.184, pp.337-351.
- [5] Grédiac M. (1989): *Principe des travaux virtuels et identification.* – Comptes Rendus de l'Académie des Sciences, vol.309, pp.1-5.
- [6] Geymonat G., Hild F. and Pagano S. (2002): *Identification of elastic parameters by displacement field measurement.* – Comptes Rendus Mécanique, vol.330, No.6, pp.403-408.
- [7] Calderon A. (1980): *On an inverse boundary value problem.* – Seminar on Numerical Analysis and its Applications to Continuum Physics, Brazilian Mathematical Society.
- [8] Claire D., Hild F. and Roux S. (2004): *A finite element formulation to identify damage fields: the equilibrium gap method.* – International Journal for Numerical Methods in Engineering, vol.61, No.2, pp.189-208.
- [9] Kavanagh K.T. and Clough R.W. (1971): *Finite element applications in the characterization of elastic solids.* – International Journal of Solids and Structures, vol.7, No.1, pp.11-23.
- [10] Roux S. and Hild F. (2018): *Optimal procedure for the identification of constitutive parameters from experimentally measured displacement fields.* – International Journal of Solids and Structures, <https://doi.org/10.1016/j.ijsolstr.2018.11.008>.
- [11] Martins J.M.P., Andrade-Campos A. and Thuillier S. (2018) : *Comparison of inverse identification strategies for constitutive mechanical models using full-field measurements.* – International Journal of Mechanical Science, vol.145, pp.330-345.
- [12] Battaglia G., Di Matteo A., Micale G. and Pirrotta A. (2018): *Vibration-based identification of mechanical properties of orthotropic arbitrarily shaped plates : Numerical and experimental assessment.* – Composites Part B, vol.150, pp.212-225.
- [13] Nguyen T.T., Huntley J.M., Ashcroft I.A., Ruiz P.D. and Pierron F. (2014): *A Fourier-series-based Virtual Fields Method for the identification of 2-D stiffness and traction distributions* – Strains, vol.50, No.5, pp.454-468.
- [14] Lubineau G., Moussawi A., Xu J. and Gras R. (2015): *A domain decomposition approach for full-field measurements based identification of local elastic parameters.* – International Journal of Solids and Structures, vol.55, pp.44-57.
- [15] Fernandez J.R., Lopez-Campos J.A., Segade A. and Vilan J.A. (2018): *A genetic algorithm for the characterization of hyperelastic materials.* – Applied Mathematics and Computation, vol.329, pp.239-250.
- [16] Goldberg D. (1989): *Genetic Algorithms in Search, Optimization, and Machine Learning.* – Addison-Wesley Professional.

- [17] Back T., Fogel D.B. and Michalewicz Z. (1997): *Handbook of Evolutionary Computation (Computation Intelligence Library)*. – 1st. Oxford University Press.
- [18] Michalewicz Z. (1996): *Genetic Algorithms+Data Structures = Evolution Programs*. – Springer Berlin Heidelberg.
- [19] Umbarkar A.J. and Sheth P.D. (2015): *Crossover operators in genetic algorithms: a review*. – ICTACT Journal on Soft Computing, vol.6, No.1, pp.1083-1092.
- [20] Cantu-Paz E. (1998): *A survey of parallel genetic algorithms*. – Calculateurs parallèles, Réseaux et Systèmes Répartis, vol.10, pp.141-171.
- [21] Gropp W., Lusk E. and Skjellum A. (2014): *Using MPI: Portable Parallel Programming with the Message-Passing Interface (Scientific and Engineering Computation)*. – The MIT Press.
- [22] Cast3M-CEA (2001) - <http://www.cast3m.cea.fr>
- [23] Oura P., Fraga B., Lopez-Novoa U. and Stoesser T. (2019): *Scalability of an Eulerian-Lagrangian large-eddy simulation solver with hybrid MPI/OpenMP parallelization*. – Computers and Fluids, vol.179, pp.123-126.

Received: June 17, 2019

Revised: September 11, 2019